Single-Ion Magnetism in Seven-Coordinate Yb^{III} Complexes with Distorted D_{5h} Coordination Geometry

Dong-Qing Wu,[a,c] Dong Shao,[a] Xiao-Qin Wei,[a] Fu-Xing Shen,[a] Le Shi,[a] Yi-Quan Zhang,*[b] Xin-Yi Wang*[a]

[a] State Key Laboratory of Coordination Chemistry, Collaborative Innovation Center of Advanced Microstructures, School of Chemistry and Chemical Engineering, Nanjing University, Nanjing, 210093, China. E-mail: wangxy66@nju.edu.cn

[b] Jiangsu Key Laboratory for NSLSCS, School of Physical Science and Technology, Nanjing Normal University, Nanjing, 210023, China

[c] School of Chemistry and Environmental Engineering, Anyang Institute of Technology, Anyang, 455000,China

Supporting Information

Table of contents

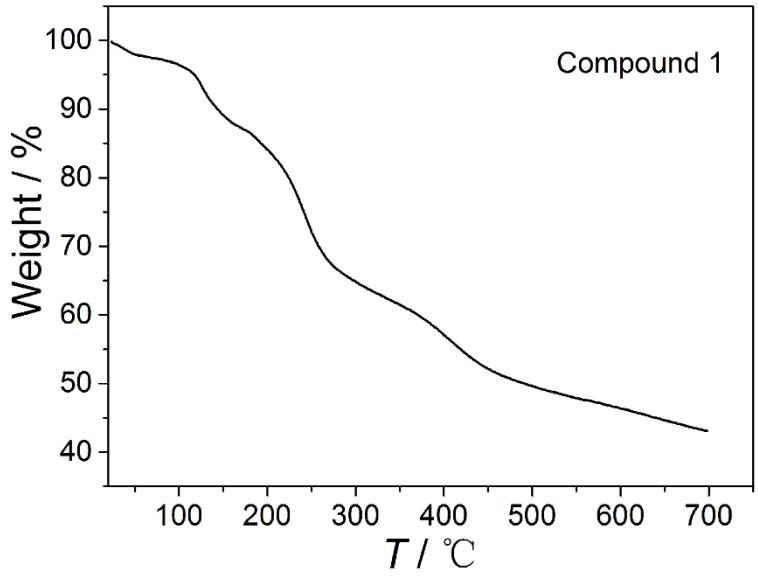

Fig. S1 TGA curve for compound **1.**

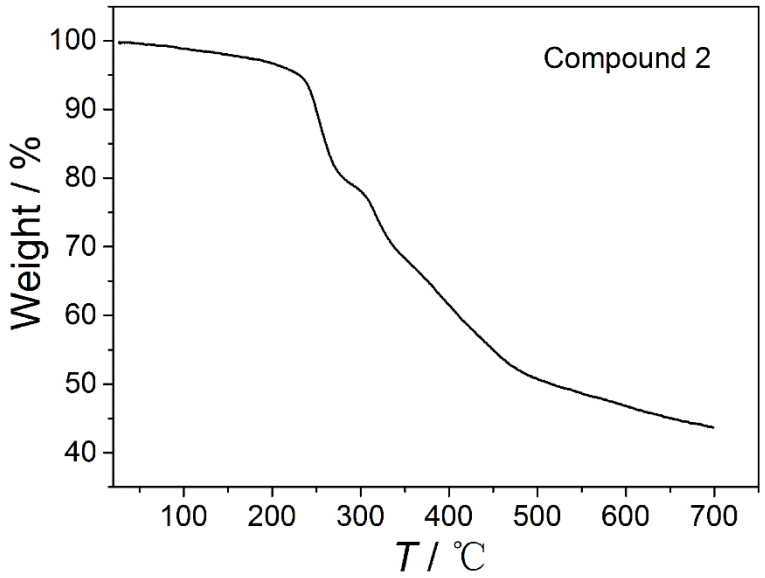

Fig. S2 TGA curve for compound **2**.

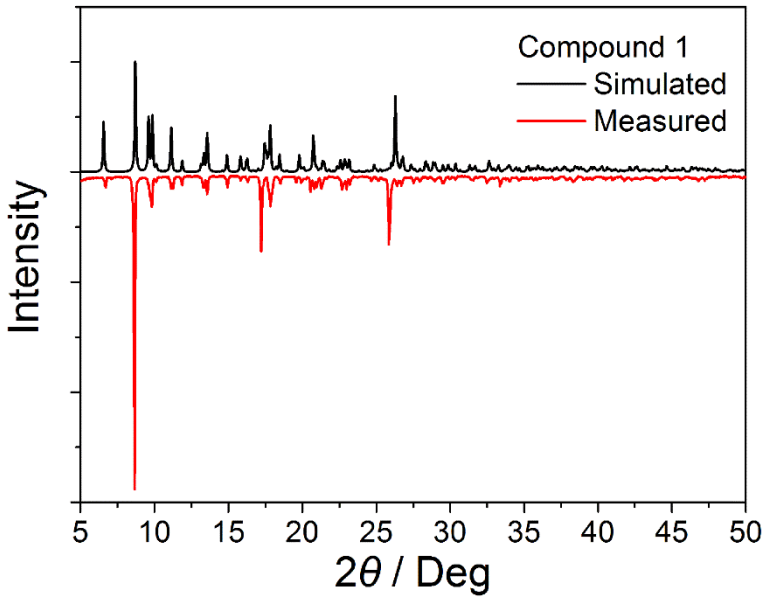

Fig. S3 Experimental and calculated PXRD patterns for compound **1**.

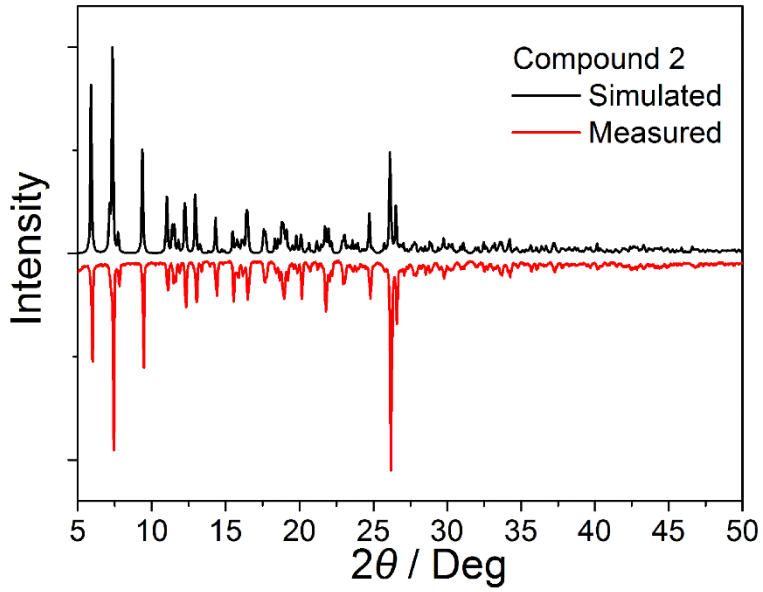

Fig. S4 Experimental and calculated PXRD patterns for compound **2**.

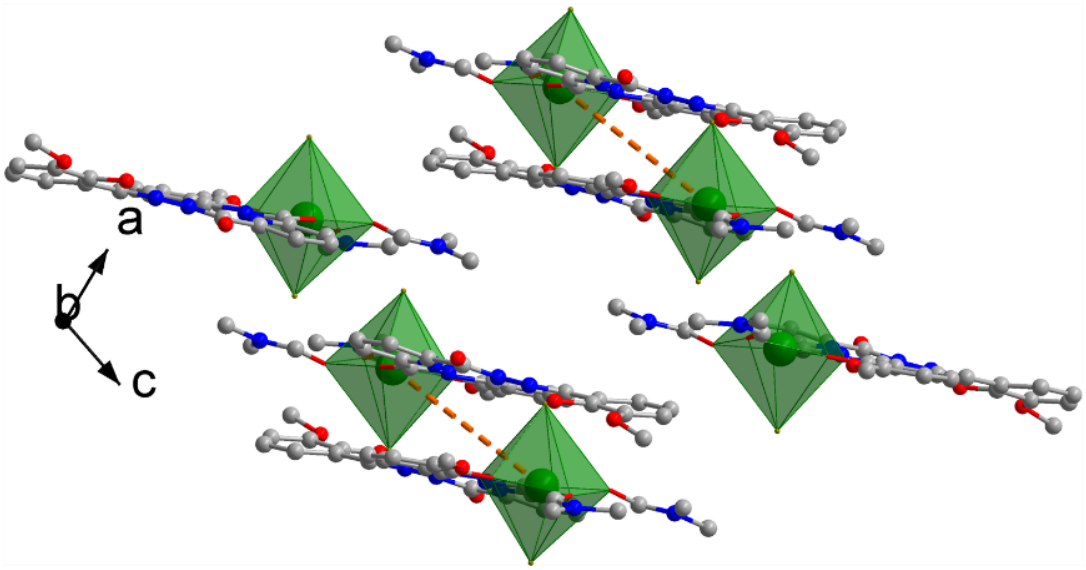

Fig.S5 Crystal packing of complex **1**. The dashed lines show the nearest intermolecular Yb···Yb separation. Hydrogen atoms and the solvents are omitted for clarity.

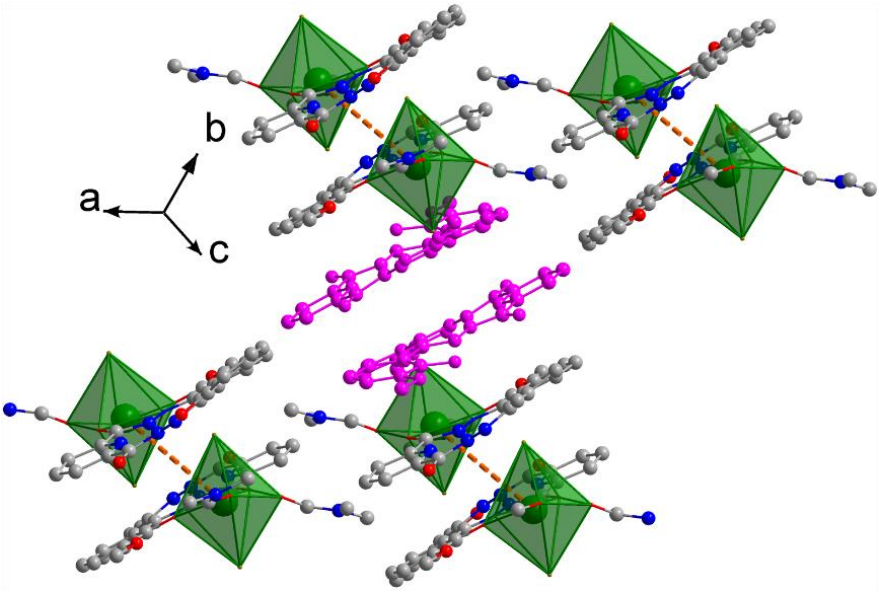

Fig.S6 Crystal packing of complex **2**. The dashed lines show the nearest Yb···Yb distances. The pink parts represent the lattice H_4bmshp molecules. Hydrogen atoms are omitted for clarity.

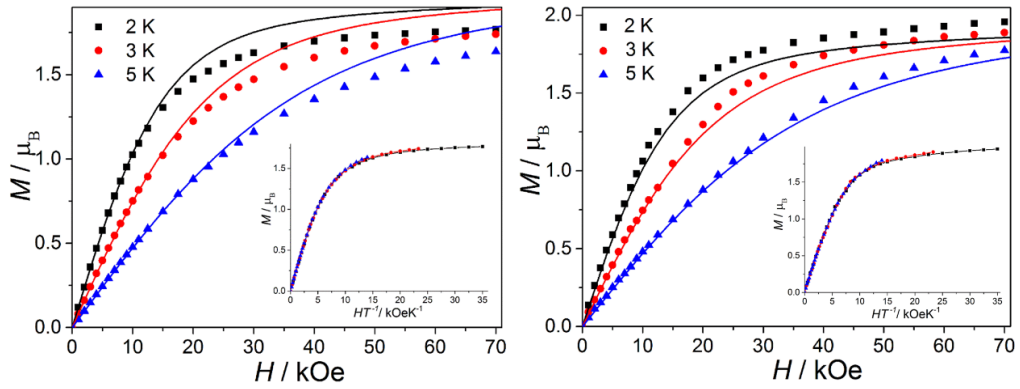

Fig.S7 The field-dependent magnetization plots at indicated temperatures for **1**(left) and **2**(right). The solid lines represent the *ab initio* calculation results. Inset: the reduced magnetization plots.

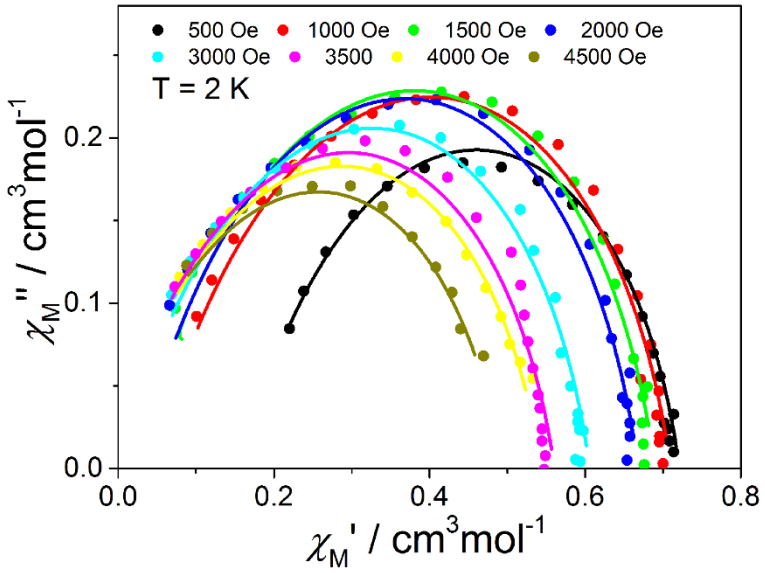

Fig. S8 Cole–Cole plots of χ'' vs. $\chi'$of **1** at 2.0 K under various applied dc fields. The solid lines represent the best fit of the experimental results with the generalized Debye model.

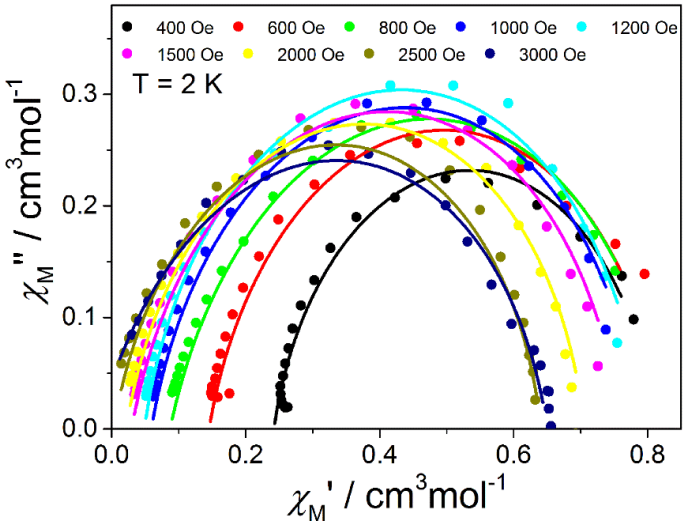

Fig. S9 Cole–Cole plots of χ'' vs. χ' of **2** at 2.0 K under various applied dc fields. The solid lines represent the best fit of the experimental results with the generalized Debye model.

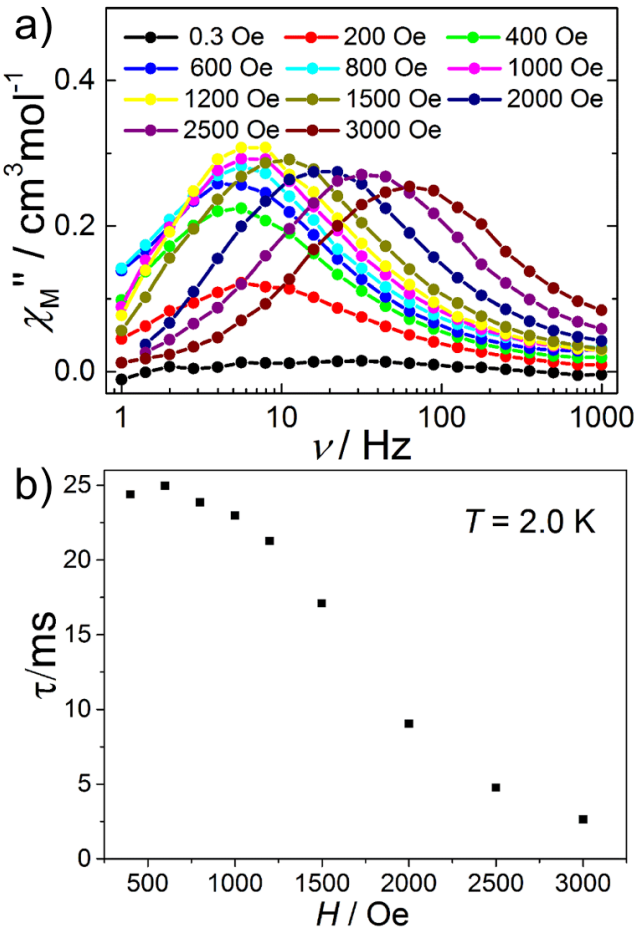

Fig.S10 (a) Frequency dependence of the out-of-phase (χ'') magnetic susceptibility of 2 (1–1000 Hz) measured at 2.0 K in various applied fields from 0 to 4500 Oe. (b) Field dependence of the magnetic relaxation time at 2.0 K for **2**.

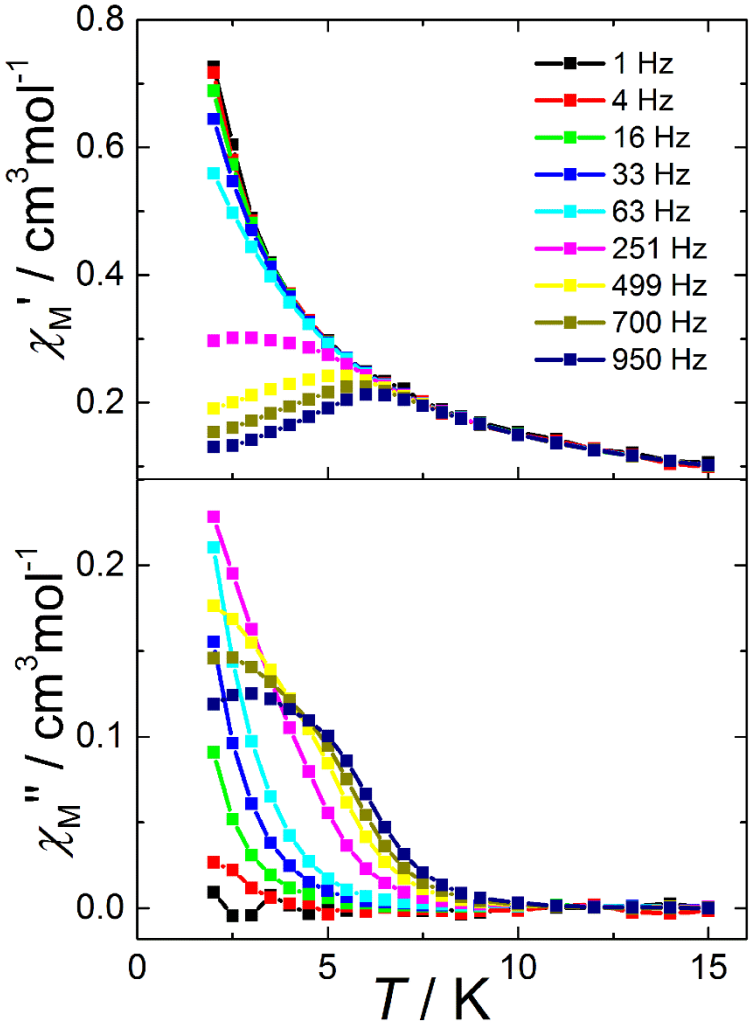

Fig. S11 Variable-temperature ac susceptibility data for **1** collected under a 1500 Oe dc field over the frequency range of 1 to 950 Hz. The solid lines are simply guides for the eye.

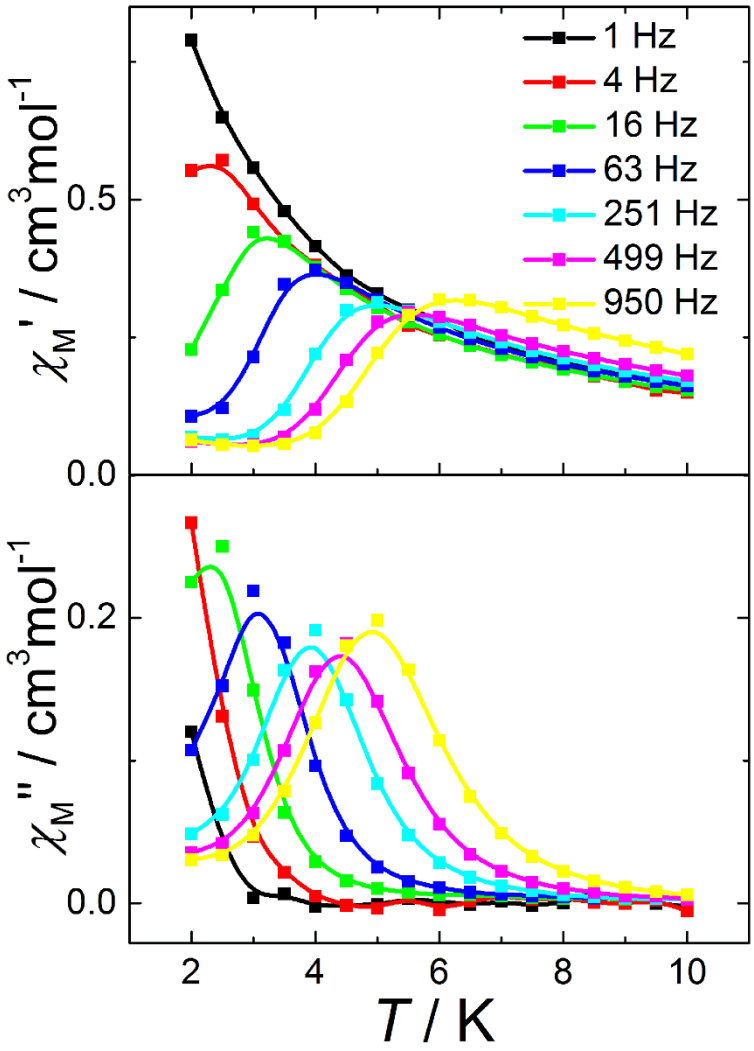

Fig. S12 Variable-temperature ac susceptibility data for **2** collected under a 600 Oe dc field over the frequency range of 1 to 950 Hz. The solid lines are simply guides for the eye.

Table S1. Selected bond lengths (Å) and bond angles (°) for **1** and **2**.

Compound 1: [Yb(H_3Bmshp)(DMF)$_2$$Cl_2$]·DMF·1.5$H_2O$					
Bond distances [Å]					
Yb(1)-O(4)	2.127(2)	Yb(1)-O(1)	2.345(2)	Yb(1)-Cl(1)	2.6662(9)
Yb(1)-O(3)	2.251(3)	Yb(1)-N(3)	2.484(3)		
Yb(1)-O(2)	2.312(2)	Yb(1)-Cl(2)	2.5781(9)		
Bond angles					
O(4)-Yb(1)-O(3)	147.84(10)	O(3)-Yb(1)-N(3)	139.37(9)	N(3)-Yb(1)-Cl(2)	84.77(7)
O(4)-Yb(1)-O(2)	76.94(9)	O(2)-Yb(1)-N(3)	148.64(9)	O(4)-Yb(1)-Cl(1)	87.78(8)
O(3)-Yb(1)-O(2)	71.97(10)	O(1)-Yb(1)-N(3)	65.32(8)	O(3)-Yb(1)-Cl(1)	90.04(9)

O(4)-Yb(1)-O(1)	137.46(9)	O(4)-Yb(1)-Cl(2)	96.66(8)	O(2)-Yb(1)-Cl(1)	100.68(8)
O(3)-Yb(1)-O(1)	74.28(10)	O(3)-Yb(1)-Cl(2)	93.37(9)	O(1)-Yb(1)-Cl(1)	86.25(7)
O(2)-Yb(1)-O(1)	145.48(9)	O(2)-Yb(1)-Cl(2)	93.73(8)	N(3)-Yb(1)-Cl(1)	83.51(6)
O(4)-Yb(1)-N(3)	72.16(9)	O(1)-Yb(1)-Cl(2)	81.17(7)	Cl(2)-Yb(1)-Cl(1)	165.54(3)
Compound 2: $[Yb(H_3Bmshp)(DMF)_2Cl_2]\cdot H_4Bmshp$					
Bond distances [Å]					
Yb(1)-O(4)	2.125(4)	Yb(1)-O(1)	2.354(4)	Yb(1)-Cl(2)	2.6250(15)
Yb(1)-O(2)	2.280(4)	Yb(1)-N(3)	2.454(4)		
Yb(1)-O(3)	2.306(4)	Yb(1)-Cl(1)	2.6088(16)		
Bond angles					
O(4)-Yb(1)-O(2)	79.00(16)	O(2)-Yb(1)-N(3)	148.93(15)	N(3)-Yb(1)-Cl(1)	88.67(11)
O(4)-Yb(1)-O(3)	147.85(18)	O(3)-Yb(1)-N(3)	138.52(16)	O(4)-Yb(1)-Cl(2)	99.39(13)
O(2)-Yb(1)-O(3)	72.53(17)	O(1)-Yb(1)-N(3)	65.76(13)	O(2)-Yb(1)-Cl(2)	86.84(13)
O(4)-Yb(1)-O(1)	137.04(14)	O(4)-Yb(1)-Cl(1)	88.88(13)	O(3)-Yb(1)-Cl(2)	93.71(14)
O(2)-Yb(1)-O(1)	143.06(15)	O(2)-Yb(1)-Cl(1)	99.78(13)	O(1)-Yb(1)-Cl(2)	80.08(11)
O(3)-Yb(1)-O(1)	74.03(16)	O(3)-Yb(1)-Cl(1)	81.68(14)	N(3)-Yb(1)-Cl(2)	89.22(11)
O(4)-Yb(1)-N(3)	71.28(14)	O(1)-Yb(1)-Cl(1)	90.43(11)	Cl(1)-Yb(1)-Cl(2)	170.31(5)

Table S2. Detailed analysis results by Contiouous Shape Measures(CShM)

Shape	Heptagon	Hexagonal pyramid	Pentagonal bipyramid	Capped octahedron	Capped trigonal prism	Johnson pentagonal bipyramid	Elongated triangular pyramid
Yb of 1	33.346	25.560	**0.865**	6.564	5.278	6.551	23.555
Yb of 2	34.337	24.593	**1.094**	6.218	4.954	6.874	21.871

Table S3. Relaxation fitting parameters from the least-square fitting of the Cole-Cole plots of compounds **1** and **2** at 2 K under various dc fields according to the generalized Debye model.

Compound **1**				
H / Oe	χ_S / $cm^3mol^{-1}K$	χ_T / $cm^3mol^{-1}K$	τ / s	α
500	0.16075	0.72103	0.00103	0.22765
1000	0.04555	0.70991	0.00112	0.23788
1500	0.02446	0.68968	0.00119	0.22833
2000	0.02579	0.66764	0.00115	0.21957
3000	0.00592	0.60565	0.00108	0.22888
3500	0.00345	0.5604	0.00105	0.24507
4000	0.00102	0.54333	0.00094	0.25192
4500	0.00227	0.49233	0.00066	0.25574
Compound **2**				
H / Oe	χ_S / $cm^3mol^{-1}K$	χ_T / $cm^3mol^{-1}K$	τ / s	α
400	0.24215	0.80742	0.02439	0.11718
600	0.14528	0.8203	0.02497	0.13837
800	0.08709	0.82194	0.02385	0.16897
1000	0.05914	0.78549	0.02296	0.13878
1200	0.0487	0.79075	0.02127	0.11788
1500	0.02967	0.75835	0.01709	0.14885
2000	0.02145	0.70516	0.00854	0.13375
2500	0.00277	0.64041	0.00426	0.13417
3000	0.00121	0.65023	0.00265	0.20213

Table S4. Relaxation fitting parameters from the least-square fitting of the Cole-Cole plots of **1** and **2** under 1.8 K-5 K according to the generalized Debye model.

Compound **1**				
Temperature / K	χ_S / $cm^3mol^{-1}K$	χ_T / $cm^3mol^{-1}K$	τ / s	α
1.8	0.07115	0.80117	0.00132	0.17814
1.9	0.05357	0.7649	0.00123	0.20234
2	0.06193	0.72939	0.00114	0.2003
2.2	0.04304	0.66223	9.4E-4	0.1871
2.4	0.0656	0.60944	8.5E-4	0.14824
2.6	0.06234	0.55823	7.4E-4	0.16812
2.8	0.08996	0.51914	6.5E-4	0.10336
3	0.06051	0.4912	5.7E-4	0.16777
3.2	0.08558	0.45478	5E-4	0.08829

3.4	0.06006	0.43615	4.3E-4	0.15456
3.6	0.07848	0.40631	4E-4	0.10911
3.8	0.06659	0.39241	3.5E-4	0.14464
4	0.07597	0.36937	3.1E-4	0.13485
4.2	0.09799	0.34947	2.9E-4	0.03006
4.4	0.07058	0.33536	2.3E-4	0.10388
4.6	0.07939	0.31887	2.1E-4	0.06729
4.8	0.08142	0.31102	1.9E-4	0.1105
5	0.09349	0.29674	1.9E-4	0.04682
Compound **2**				
Temperature / K	χ_S / $cm^3mol^{-1}K$	χ_T / $cm^3mol^{-1}K$	τ / s	α
1.8	0.06457	0.91371	0.03628	0.16728
2	0.05695	0.8152	0.02489	0.16816
2.2	0.04807	0.73223	0.0174	0.14201
2.4	0.05423	0.68507	0.01271	0.12498
2.6	0.04306	0.60895	0.00787	0.09563
2.8	0.04251	0.56552	0.00553	0.0889
3	0.03147	0.57441	0.00389	0.08944
3.2	0.02967	0.4906	0.00238	0.07199
3.4	0.02796	0.46026	0.00163	0.05293
3.8	0.00642	0.42769	8.1E-4	0.07681
4	0.00399	0.39634	5.4E-4	0.05556
4.2	0.00783	0.38507	3.9E-4	0.07149
4.4	0.02674	0.36457	2.8E-4	0.06106
4.6	0.00258	0.35551	2.3E-4	0.03
4.8	0.03749	0.34806	2E-4	0.06068
5	0.01596	0.33323	1.4E-4	0.05419

Table S5. Parameters fitted from the Arrhenius plots in Fig.6 considering multiple relaxation processes

Compound **1**			
	Value	Standard error	R^2
A	368.14	12.93	0.99
C	12.24	2.92	
n	3.62	0.15	
Compound **2**			
	Value	Standard error	R^2
A	10.22	0.95	0.99
C	0.38	0	
n	5.60	0.12	
τ_0	5.77E-7	0	
U_{eff}	30.43	0.75	

Table S6. Calculated energies and wave functions with definite projection of the total moment |JM > for the lowest four Kramers doublets (KDs) of Yb^{III} fragments in compounds **1**–**2**.

	***E*/cm^{-1}**	**wave functions**
1	0.0	99%|±1/2>
	197.7	84|±3/2>+13%|±5/2
	421.1	19%|±7/2>+69%|±5/2>+12%|±3/2>
	543.5	77%|±7/2>+18%|±5/2>
2	0.0	62%|±7/2>+30%|±3/2>+5%|±1/2>
	187.0	9%|±7/2>+60%|±5/2>+5%|±3/2>+26%|±1/2>
	381.0	15%|±7/2>+27%|±5/2>+21%|±3/2>+37%|±1/2>
	457.7	15%|±7/2>+9%|±5/2>+44%|±3/2>+32%|±1/2>

Table S7. Calculated energy levels (cm^{-1}), $\boldsymbol{g}$ (g_x, g_y, g_z) tensors and m_J values of the lowest Kramers doublets (KDs) of the Yb^{III} fragments of compounds **1**–**2**.

KDs	**1(Yb_1)**			**3(Yb_2)**		
	E/cm^{-1}	$\boldsymbol{g}$	m_J	*E*/cm^{-1}	$\boldsymbol{g}$	m_J
1	0.0	4.875 4.120 1.095	±1/2	0.0	0.888 2.854 5.727	±7/2
2	197.7	1.785 1.920 3.664	±3/2	187.0	0.841 2.211 4.061	±5/2
3	421.1	1.102 2.896 5.003	±5/2	381.0	0.994 2.969 5.144	±1/2
4	543.5	0.687 0.969 7.479	±7/2	457.7	0.876 1.244 7.016	±3/2

Table S8. *Ab initio* calculated crystal-field parameters for the investigated compounds **1**–**2**.[a]

		B(*k*,*q*)	
k	***q***	**1**	**2**
2	–2	0.1790×10^{1}	0.3899×10^{1}
2	–1	0.7419×10^{1}	-0.4266×10^{-1}
2	0	$\mathbf{0.12741\times10^{2}}$	-0.5277×10^{1}
2	1	-0.67245×10^{1}	-0.1602×10^{1}
2	2	0.3841	0.1473×10^{2}
4	–4	–0.1081	0.8364×10^{-1}
4	–3	0.1141	0.5015×10^{-2}
4	–2	0.9297×10^{-1}	-0.5019×10^{-1}
4	–1	0.1016	0.5316
4	0	–0.1358	-0.1025×10^{-1}
4	1	–0.1597	0.4306×10^{-1}
4	2	0.2501	0.7658
4	3	0.2451	–0.1044
4	4	–0.6925	–0.2964
6	–6	0.9408×10^{-4}	-0.4436×10^{-2}
6	–5	0.5269×10^{-2}	-0.8132×10^{-1}
6	–4	0.3820×10^{-2}	0.4574×10^{-3}
6	–3	0.2182×10^{-2}	0.8781×10^{-2}
6	–2	-0.1640×10^{-3}	0.1736×10^{-3}
6	–1	-0.6440×10^{-2}	-0.6961×10^{-2}
6	0	0.3147×10^{-2}	-0.1206×10^{-2}
6	1	0.5682×10^{-4}	0.2771×10^{-2}
6	2	0.1168×10^{-1}	0.1167×10^{-1}
6	3	0.7592×10^{-2}	0.4136×10^{-2}
6	4	-0.9253×10^{-4}	-0.6725×10^{-2}
6	5	-0.7073×10^{-2}	-0.6472×10^{-2}
6	6	-0.6762×10^{-2}	0.2257×10^{-1}

[a]Only the ranks k = 2, 4, and 6 are shown; higher ranks are much smaller and are not shown here.